7. J. Kinugawa, M. Ochiai, C. Matsumura, and H. Yamamoto, *ibid.*, **12**, 433 (1964).
8. K. L. Vieira and D. G. Peters, *J. Electroanal. Chem.*, **196**, 93 (1985).
9. C. E. Dahm and D. G. Peters, *Anal. Chem.*, **66**, 3117 (1994).
10. J. A. Cleary, M. S. Mubarak, K. L. Vieira, M. R. Anderson, and D. G. Peters, *J. Electroanal. Chem.*, **198**, 107 (1986).

11. L. W. Marple, *Anal. Chem.*, **39**, 844 (1967).
12. C. W. Manning and W. C. Purdy, *Anal. Chim. Acta.*, **51**, 124 (1970).
13. M. S. Mubarak, D. D. Nguyen, and D. G. Peters, *J. Org. Chem.*, **55**, 2648 (1990).
14. S. Zhan and M. D. Hawley, *J. Electroanal. Chem.*, **319**, 275 (1991).
15. H. W. VandenBorn and D. H. Evans, *J. Am. Chem. Soc.*, **96**, 4296 (1974).

Magnetic Field Effects on Nickel Electrodeposition

O. Devos,[a] A. Olivier,*,[a] J. P. Chopart,[a] O. Aaboubi,[a] and G. Maurin[b]

[a] *CNRS, EP 120 "Dynamique des Transferts aux Interfaces," UFR Sciences, 51687 Reims, France*
[b] *CNRS, UPR 15 "Physique des Liquides et Electrochimie," 75252 Paris, France*

ABSTRACT

The effects of a superimposed magnetic field **B** on the structure of nickel electrodeposits prepared from a quiescent Watts solution were studied by scanning electron microscope and transmission electron microscopy investigations. It was observed that **B** can induce a change of the surface morphology and of the preferential growth direction of the nickel grains. In the absence of organic inhibitor, it is shown that these effects result from an inhibition of nickel electrocrystallization in relation to the mass-transport enhancement of H^+ ions promoted by the magnetic field. The phenomenon is much more important in the presence of a strong inhibitor such as 2-butyne-1,4-diol, the activity of which is also under mass-transport limitation. The presence of the magnetically induced convective flow is directly illustrated by the perturbations of the relief of the deposit in the vicinity of attached bubbles. These results demonstrate that most structural modifications of nickel electrodeposits observed in the presence of a magnetic field are consequences of convection phenomena induced by a magnetohydrodynamic effect.

Introduction

According to several review papers, an imposed magnetic field presents various effects on electrolytic processes and in particular on the morphology and structure of metals or alloys prepared by electrodeposition.[1,2] For example, It was observed that the shape of zinc or lead dendrites grown by electrodeposition can be strongly modified in the presence of a magnetic field and that, in some cases, the dendritic growth can be totally inhibited to give smooth deposits, with an increase of the metal deposition efficiency.[3-5]

These results are currently attributed to the Lorentz force exerted by the electromagnetic field **B** on the ions of charge q moving at the velocity **v** within an electric field **E**[2]

$$\mathbf{F} = q \, (\mathbf{E} + \mathbf{v} \times \mathbf{B}) \qquad [1]$$

During the electrolysis, the Lorentz force would induce a convective flow of the electrolytic solution. Therefore, the resulting mass-transport enhancement can reduce or suppress the usual consequences of the diffusion control, such as the strong tendency to form dendritic outgrowths. The magnetohydrodynamic (MHD) effect on mass-transport has been evaluated by measuring the limiting current of various electrochemical processes. Several semi-empirical expressions of the dependence of i_L vs **B** were derived.[6-9] It is generally admitted that i_L is proportional to $\mathbf{B}^{1/3}$.

It has also been suggested that magnetic fields could have kinetic effects by inducing an overpotential, by decreasing the hydration number of cations, or by modifying chemisorption at the interface.[3,10,11] However, Fricoteaux et al.,[12] by using radiotracer elements, demonstrated that the apparent current exchange variations which were experimentally observed during copper electrodeposition in the presence of an imposed magnetic field would result from modifications of the morphology of the metallic coating.

Here, an experimental investigation is presented, of the effects of a magnetic field on the structure and on the preferred growth orientation of nickel electrodeposits prepared from a Watts bath which contained, in some cases, small quantities of a strong organic inhibitor.

In an early paper, Yang[13] studied the influence of the deposition parameters on the fiber axis of Ni, Fe, or Co electrodeposits by using reflection high-energy electron diffraction (RHEED). He concluded that an imposed magnetic field had no significant effect on their preferred orientations. Chiba et al.[3] observed minor variations in the quality of the preferred orientations of nickel electrodeposits especially when deposits were prepared at low current density. These authors suggested that **B** could modify the crystal growth orientations in relation to the easy magnetic axis. This effect would be more pronounced at low current densities, where the influence of the magnetic field would be larger than that of the electric field.

In spite of these contradictory results, nickel electrodeposition from a concentrated electrolyte such as the usual Watts bath appears to be a good experimental system for the identification of the specific effects of a magnetic field on electrocrystallization, owing to the considerable amount of knowledge which has been accumulated. It is known that the overall deposition rate is governed by interfacial reactions;[14] thus, nickel ion transport has practically no influence on the deposition process. Moreover, the specific structures and surface morphologies of all textures were identified.[15,16] The growth axis of the grains depends on operational parameters such as the pH of the bath and the applied potential. For example, in the Watts bath and for moderately acidic pH, four growth textures are successively observed when the potential is moved toward more negative values: the <110> texture at very low current density, the <211> texture at low current density, the <100> texture for medium and high current density, and finally a second <110> texture for a very high current density. It was demonstrated that the direction of preferential growth is determined by a competitive adsorption of various species (especially hydrogen species) on the crystal faces of the growing nickel crystals.[17,18] Therefore, the texture axis as well as the microstructure of nickel coatings is very sensitive to any modification of the state of adsorption, resulting, for example, from the addition of small quantities of organic compounds, or from the use of pulsed currents,[19] and they can be considered to be a sensitive test for the detection of an effect of a magnetic field.
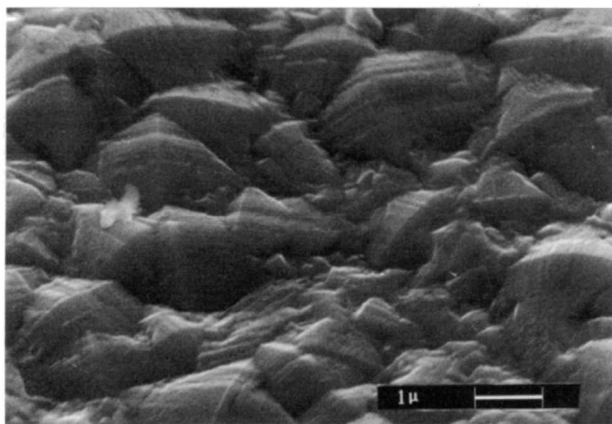
* Electrochemical Society Active Member.

Fig. 1. SEM image of a nickel electrodeposit prepared at −0.800 V/SCE in a pure Watts solution in the presence of magnetic field. (*B* = 0.6 T) Characteristic morphology of a <211> texture.

Experimental

Nickel thin films (typically 10 μm thick) were electrodeposited under potentiostatic control on a horizontal titanium substrate (area = 1 cm²) from a quiescent Watts solution (NiSO$_4$ 7H$_2$O 300 g/l, NiCl$_2$, 6H$_2$O 35 g/l, H$_3$BO$_3$ 40 g/l; pH 4.5) maintained at 30 °C. The counterelectrode was a large planar nickel sheet parallel to the cathode. The 100 cm³ cell was plunged in a uniform magnetic field (up to 1.0 T) delivered by an electromagnet (Drusch EAM 20G). **B** was parallel to the electrode surface. Most experiments were carried out in two potential ranges, −0.800 V/SCE (with respect to a saturated calomel reference electrode), and −0.920 to −1.1 V/SCE, respectively. The first potential corresponds precisely to the transition between the <211> and the <100> preferred orientations. The second potential range corresponds to the experimental domain where a strong <100> texture is established. In a full set of experiments, small amounts (typically 5 × 10^{-3} M) of 2-butyne-1,4-diol, an organic additive which is known to be a strong brightener,[21] were added to the Watts solution.

The preferred orientations of the deposits were determined by X-ray powder diffraction and by RHEED. The morphology was studied by SEM, and the microstructure was observed by TEM.

Results

Nickel electrodeposition in pure Watts solution.—At a low cathodic potential (*V* = −0.800 V/SCE), in the absence of magnetic field, X-ray diffraction (XRD) diagrams indicated that nickel deposits exhibit a mixture of weak <211> and weak <100> textures. This structure was also identified on the SEM images, where the characteristic morphologies of the two textures, which are randomly distributed, are easily recognized. When a magnetic field was superimposed, the current density decreased slightly (a few percent), and the <211> preferred orientation became predominant as compared to the <100> texture. For example, for a magnetic induction *B* = 0.6 T, most grains had a

lozenge shape which is characteristic of the <211> growth texture (Fig. 1). The quality of this texture increases with the intensity of the applied magnetic field.

At a more negative potential (−1.0 to −1.1 V/SCE), a very strong <100> preferred orientation was revealed by a single sharp [200] diffraction peak on the XRD diagrams (Fig. 5a). The superimposition of the magnetic field (0.1 to 1 T) had no significant effect on the preferred orientation (Table I). On Fig. 2, one can observe that the RHEED diagram which is characteristic of a good <100> texture is symmetric with respect to the normal of the surface. There is no evidence that the preferential growth direction, indicated by the position of the [200] spot on the diffraction diagram, would be distorted by the magnetic field. The characteristic grain morphology, irregular square pyramids (Fig. 3), as well as the internal grain structure (Fig. 4) as observed by TEM are not affected by the magnetic field. Few oblique {111} stacking faults were observed, as usual.

Nickel electrodeposition in the presence of 2-butyne-1,4-diol.—The effects of the magnetic field became very significant when a few 10^{-3} M of this organic inhibitor were added to the Watts electrolyte. They were particularly spectacular for deposits prepared under a very negative potential (−0.920 to −1.100 V/SCE). The first consequence was a significant decrease (25% for **B** = 0.78 T) of the current intensity, which is symptomatic of the inhibition of the growth kinetics. But the effect on the structure of the deposit was even more evident. In Fig. 5, one can observe the evolution of the XRD diagrams for a constant inhibitor concentration (c = 5 × 10^{-3} M) and for increasing value of the magnetic field intensity. For **B** = 0, as mentioned above, a sharp and intense [200] peak indicates a strong <100> texture. For **B** = 0.3 T, this texture is drastically weakened, and the presence of the other diffraction peaks reveals the apparition of a mixture of a weak <100> texture with a weak <110> texture (Fig. 5b). For more intense magnetic fields, the <110> texture revealed by the [220] peak becomes predominant and more intense, whereas the other textures completely disappear (Fig. 5c and d), as for a nickel deposit prepared on a rotating disk electrode (Table I).[18] The inhibition effect by the 2-butyne-1,4-diol was so intense in the presence of *B* ≥ 0.6 T that the nickel surface became very bright and it was no longer possible to identify the morphology of the individual grains (Fig. 8). However, on TEM images, the specific features of the textures are still well apparent. In particular, for deposits prepared in the presence of an intense magnetic field, the mean grain size *d* was drastically reduced (from *d* ≈ 2 μm for *B* = 0 to *d* ≈ 0.07 μm for *B* = 0.9 T). Nevertheless, the arrangement of parallel vertical twin planes, which is characteristic of the <110> texture,[20] was still visible in all grains (Fig. 6).

*Effect of **B** on bubble tracks.*—A dramatic effect of the magnetic field during nickel electrodeposition involves the shape of the pits usually observed on the surface of the metallic coating, which are due to the attachment of bubbles resulting from hydrogen evolution. In the absence of any forced convection (quiescent electrolyte, no magnetic field), the bubble pits had the appearance of spherical caps with a perfectly circular rim even in the presence of

Table I. Schematic presentation of the texture domains of nickel electrodeposits prepared from a Watts electrolyte at 30 °C in various experimental conditions.
Abbreviations: BD = 5 × 10^{-3} M 2-butyne-1,4-diol; VS = very strong, S = strong, M = medium, W = weak.

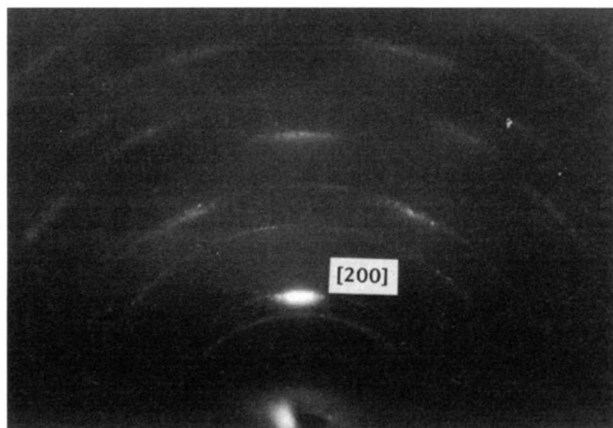| Potential	→ (V/ECS)	−0.7	−0.8	−0.9	−1.0	−1.1
Quiescent	B = 0	-W <211> + W <100>		-----------VS <100>--------		
Pure Watts sol.	B ≠ 0	---M <211>-	W <100>	-----------VS <100>--------		
Quiescent	B = 0	---M <211>--	W <100>	-----------S <100>--------		
Watts solution + BD	B = 0.3 T	-----W <110> + W <100>---------------------				
	B = 0.6 T	--------M <110>---------------------------				
	B = 0.9 T	-------S <110>---------------------------				
Watts solution + BD on a RDE	B = 0	-----------S <110>------------------------				

Fig. 2. RHEED pattern of a nickel electrodeposit prepared at −1.1 V/SCE in a pure Watts solution in the presence of magnetic field (*B* = 0.6 T). Typical <100> texture diagram.
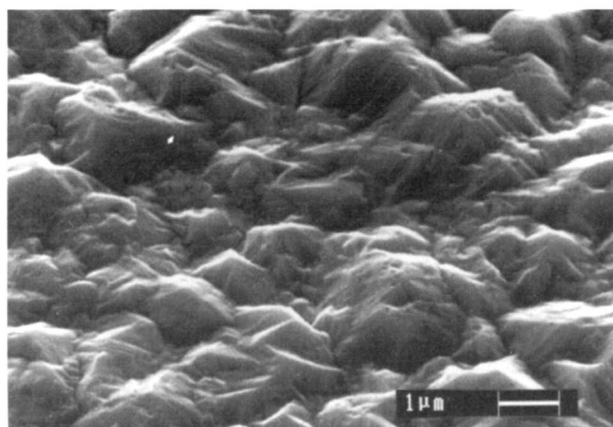

Fig. 5. X-ray diffraction diagrams of nickel electrodeposits prepared at −1.00 V/SCE from a Watts solution containing 5 × 10^{-3} M 2-butyne-1,4-diol for various intensities of the superimposed magnetic field. (Mo K$_\alpha$ X-ray source, vertical axis in a square root scale). a– B = 0: very strong <100> texture; b– B = 0.3 T: mixture of <100> and <211> textures; c– B = 0.6 T: medium <110> texture; and d– B = 0.9 T: strong <110> texture.

Fig. 3. SEM image of a nickel electrodeposit prepared at −1.00 V/SCE in a pure Watts solution. This characteristic morphology of the <100> texture is independent of the presence of a magnetic field.

Fig. 6. Transmission electron micrography of a nickel electrodeposit prepared at −1.0 V/SCE from a Watts electrolyte containing 5 × 10^{-3} M 2-butyne-1,4-diol in the presence of magnetic field (B = 0,9T). Very small grains with the characteristic structure of the <110> texture.

2-butyne-1,4–diol (Fig. 7). In the simultaneous presence of the inhibitor and a magnetic field, the shape of the bubble pits was completely modified. The rim of the depression was no longer circular, and a long "tail" normal to the direction of **B** became apparent (Fig. 8). The length of this tail, which increased with **B** and the current intensity, reached several millimeters, sufficiently long to be visible to the naked eye on bright electrodeposits. From SEM

observations at a low incidence angle, it appeared that this tail is a narrow depression on the nickel surface. Conversely, at the opposite side of the bubble pit, an overthickness was always present. It is evident that these features come from an enhancement of the inhibition along the tail and a decrease of it on the overthickness. This phe-
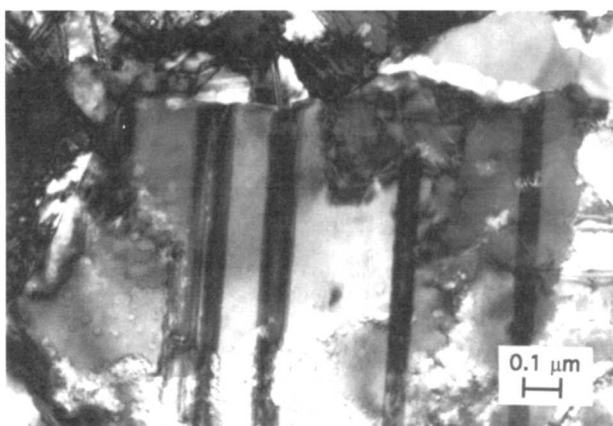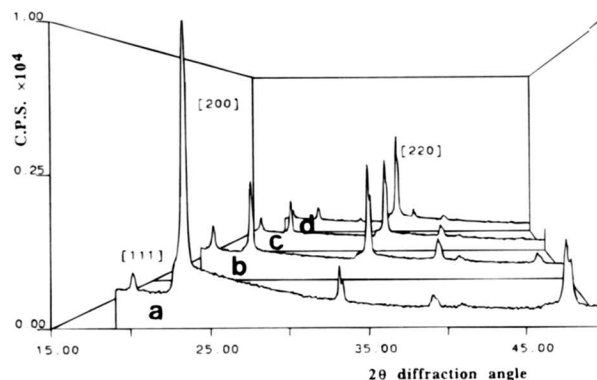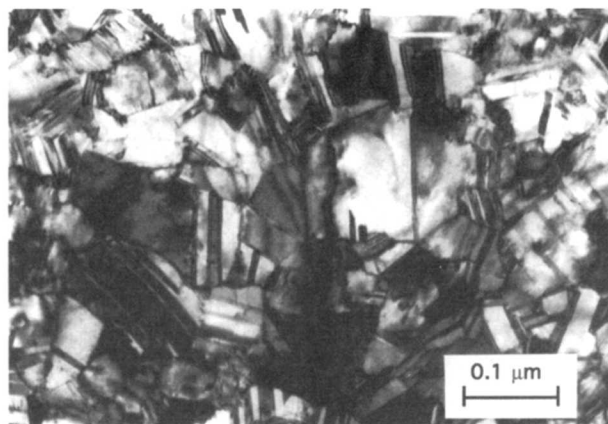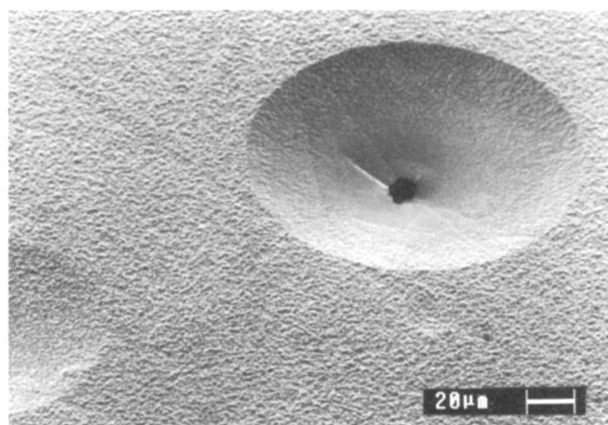

Fig. 4. Transmission electron micrography of a nickel electrodeposit prepared from a pure Watts electrolyte at −1.0 V/SCE. Typical grain structure for the <100> texture observed indifferently in the absence or in the presence of a magnetic field.

Fig. 7. SEM image of a bubble track on a stationary nickel deposit prepared at V = −1.1 V/SCE from a Watts electrolyte containing 5 × 10^{-3} M 2-butyne-1,4-diol in the absence of magnetic field.
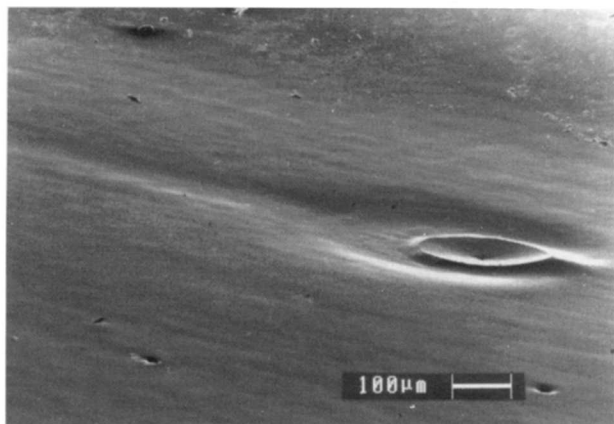
Fig. 8. Bubble track on a stationary nickel deposit prepared at -1.00 V/SCE from a Watts electrolyte containing 5×10^{-3} M 2-butyne-1,4-diol in the presence of a magnetic field ($B = 0.6$ T).

Fig. 10. Schematic representation of the convective electrolyte flow in the vicinity of an attached hydrogen bubble. The inhibition effect of the organic additive is reduced on the front side and below the bubble where it is enhanced by the turbulent drag behind the bubble.

nomenon is very similar to that commonly observed on nickel electrodeposits prepared on a rotating disk electrode in the presence of an inhibitor like 2-butyne-1,4-diol (Fig. 9). The only difference is that, in the last case, the tail was not rectilinear but had a helical shape. In both cases, the features result from the forced convection of the electrolyte along the electrode surface. The inert spherical body constituted by an attached bubble induces behind it a turbulent drag which enhances the transport of the inhibitor toward the nickel surface and therefore reduces the growth rate. Conversely, as illustrated in Fig. 10, on the front side of the bubble, the deviation of the stream creates a stagnation point which reduces locally the effect of the inhibitor. This reduction can be sufficient to cancel the texture change. In this case, one can observe on the overthickness the morphology of the <100> texture, which is characteristic of the weakness of inhibition. The same phenomenon occurs on the rim of the pit, where the liquid blocked under the bubble is practically motionless.

In the absence of inhibitor, the effect of **B** on the bubble tracks is negligible in the full potential range. At very negative potential, the faradaic efficiency is close to 100%, and the crystal growth is independent of the electrolyte flow. At low or moderate potential (V > -0.9 V/SCE), the MHD effects are expected to be weak because of the low current density. Nevertheless, in a few cases, we observed behind the bubble pit (with respect to the **B** direction) a small variation of the surface morphology which can also be attributed to a local enhancement of the flow rate.
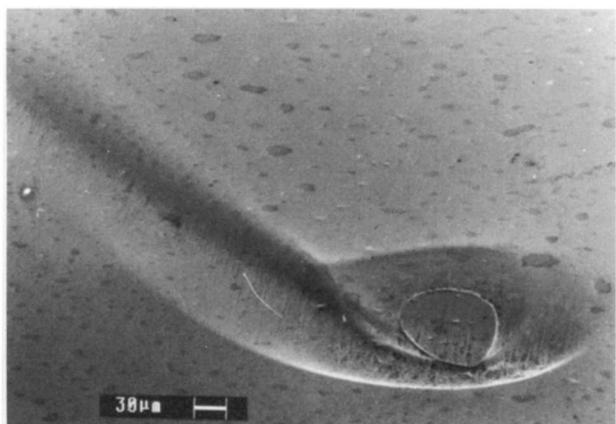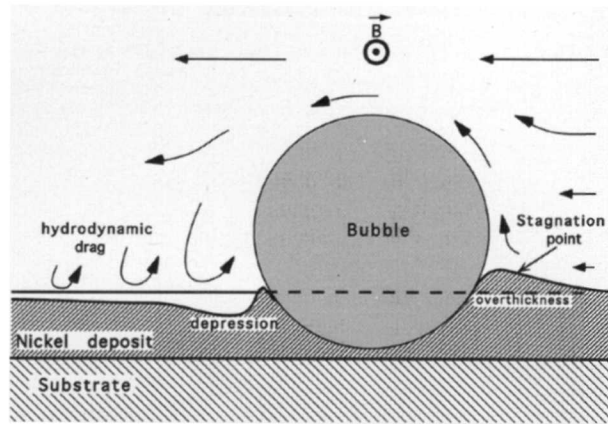
Discussion

The data presented here demonstrate that a superimposed magnetic field parallel to the substrate can disturb the structure and the morphology of nickel electrodeposits, especially when they are prepared in the presence of an inhibitor, even though the reduction rate is not under mass-transport control of Ni^{2+} ions. One might deduce that the magnetic field would be involved in the exchange process at the interface or would modify the crystal growth pattern according to the easy axis of magnetization of this metal, as was previously suggested.[3,10] In fact, in agreement with our knowledge on the electrocrystallization mechanism, it appears that **B** acts indirectly on nickel electrodeposition through the perturbation of secondary processes, namely, the hydrogen evolution and the inhibitor adsorption.

During the nickel electrodeposition, a part of the current is consumed by the hydrogen evolution reaction. At low or moderate overpotential, the partial hydrogen current i_H is under the diffusion control of H^+ ions, and therefore the faradaic efficiency of nickel electrodeposition depends on the total current and on the hydrodynamic conditions.[22,23] In the absence of forced convection, the surface concentration of hydrogen species is reduced to zero. In other respects, according to Amblard et al.,[17] the preferential growth of nickel along a <211> or a <110> axis is determined by the specific adsorption at the interface respectively, of $Ni(OH)_2$ and atomic hydrogen H_{ads}. Since $Ni(OH)_2$ comes from the interfacial pH shift, these two adsorbed species are provided by the hydrogen reduction reaction. The transition from the <100> texture into the <211> texture and the small decrease of the current intensity which were observed at -0.8 V/SCE under the effect of **B** are therefore ascribed to the increase of the surface inhibition owing to the larger mass transport of H^+ ions thanks to the MHD effect. However, the current intensity decrease was too small to evaluate its dependence vs B. It is worth noting that another perturbation method of the adsorption/desorption equilibrium includes the use of pulsed current. During the rest times, the inhibiting species H_{ads} or $Ni(OH)_2$ can desorb, and a correlative transition of the texture was observed,[19] in agreement with the interpretation of the control of the textures by the surface inhibition.

In the presence of 2-butyne-1,4-diol, a similar process is involved. This acetylenic alcohol is consumed at the cathodic interface by the catalyzed hydrogenation of the $-C \equiv C-$ unsaturated bond. The surface concentration of this compound at the cathode is controlled by mass transport and can be reduced to zero in the absence of convection. The structural changes which were observed as soon as a magnetic field was applied are due to the enhance-

Fig. 9. Bubble track on a bright nickel deposit prepared on a rotating disk electrode ($\Omega = 2000$ rpm) from a Watts solution containing 1×10^{-3} M 2-butyne-1,4-diol. Note the helical tail.

ment of the transport of the inhibitor toward the cathode by MHD convection and are in agreement with the texture diagram of Ref. 18, which was obtained with a rotating disk electrode. As described above, the effect is even more visible in the vicinity of attached bubbles. The perturbation of the convective flow by these obstacles modifies the distribution of the surface concentration of the inhibitor. In particular, in the turbulent drag behind the obstacle, the component of the flow velocity normal to the surface increases the rate of arrival of the organic compound and reduces locally the nickel growth rate, creating a depression.

Conclusion

In this study, all the observed structural and morphological changes result from the increase of the surface concentration of inhibiting species caused by the mass-transport enhancement by the MHD effect.[24] There is no evidence of any effect on the kinetics of nickel electrodeposition, although this hypothesis can not be totally excluded. However, the mechanism by which the MHD forces are able to induce a convection of the liquid phase is complex. According to a new model which is derived by Chopart et al.,[25] these forces result from the interaction between the magnetic field and the intense electric field.[26] They are developed in the narrow region of the diffuse layer, where the overall electric charge differs from zero and also where the adsorption phenomena are localized. The convective flow generated by these processes is extended by viscous effects at a distance from the surface by at least the order of magnitude of the bubble diameter ($\approx$200 μm), as is demonstrated by the deformation of the bubbles.

REFERENCES

1. T. Z. Fahidy, *J. Appl. Electrochem.*, **13**, 553 (1983).
2. R. A. Tacken and L. J. J. Janssen, *ibid.*, **25**, 1 (1995).
3. A. Chiba, T. Nimi, H. Kitayama, and T. Ogawa, *Surf. Coat. Technol.*, **29**, 347 (1986).
4. A. Chiba and T. Ogawa, *Chem. Abstr.*, **108**, 175,888 (1988).
5. I. Mogi, M. Kamiko, and S. Okubo, *Physica B*, **211**, 319 (1995).
6. T. Z. Fahidy, *Electrochim. Acta*, **35**, 929 (1990).
7. J. Lee, S. R. Ragsdale, X. Gao and H. S. White, *J. Electroanal. Chem.*, **422**, 169 (1997).
8. R. Aogaki and K. Fueki, *This Journal*, **131**, 1295 (1984).
9. O. Aaboubi, J. P. Chopart, J. Douglade, A. Olivier, C. Gabrielli, and B. Tribollet, *ibid.*, **137**, 1796 (1990).
10. J. K. Kelly, *ibid.*, **124**, 987 (1977).
11. A. Danilyuk, V. Kurmashev, and A. Matyryushlov, *Thin Solid Films*, **189**, 247 (1990).
12. P. Fricoteaux, A. Olivier, and R. Delmas, *This Journal*, **139**, 1096 (1992).
13. L. Yang, *ibid.*, **101**, 456 (1954).
14. I. Epelboin and R. Wiart, *ibid.*, **118**, 1577 (1971).
15. I. Epelboin, M. Froment, and G. Maurin, *Plating*, **56**, 1356 (1969).
16. G. Maurin, Ph.D. Thesis, Paris VI (1970); *Oberflásche Surf.*, **11**, **12** (1970); *ibid.*, **1**, **2**, **3** (1971).
17. J. Amblard, M. Froment, and N. Spyrellis, *Surf. Technol.*, **5**, 205 (1977).
18. J. Amblard, I. Epelboin, M. Froment, and G. Maurin, *J. Appl. Electrochem.*, **9**, 233 (1979).
19. C. Kollia, N. Spyrellis, J. Amblard, M. Froment, and G. Maurin, *ibid.*, **20**, 1025 (1990).
20. J. Amblard, M. Froment, G. Maurin, and N. Spyrellis, *J. Microsc. Spectrosc. Electron.*, **6**, 311 (1981).
21. M. Froment, G. Maurin, and J. Thevenin, *C. R. Acad. Sci., Paris*, **266**, 1125 (1968).
22. R. K. Dorsch, *J. Electroanal. Chem.*, **21**, 495 (1969).
23. C. Arkam, V. Bouet, C. Gabrielli, G. Maurin, and H. Perrot, *This Journal*, **141**, L103 (1994).
24. O. Devos, A. Olivier, J. P. Chopart, O. Aaboubi, and G. Maurin, Abstract 462, p. 561, The Electrochemical Society Meeting Abstracts, Vol. 97-2, Paris, France, Aug. 31-Sept. 5, 1997.
25. J. P. Chopart, O. Devos, O. Aaboubi, E. Merienne, and A. Olivier, in *Proceedings of the 3rd International Conference on Transfer Phenomena in Magnetohydrodynamic and Electroconducting Flows*, Aussois, France, p. 69 (1997).
26. E. Tronel-Peyroz and A. Olivier, *Phys. Chem. Hydrodyn.*, **3**, 251 (1982).